2018 IEEE/RSJ International Conference on Intelligent Robots and Systems (IROS)
Madrid, Spain, October 1-5, 2018

Neurorobotic approach to study Huntington disease based on a mouse neuromusculoskeletal model

Satoshi Oota[1], Yuko Okamura-Oho[2], Ko Ayusawa[3], Yosuke Ikegami[4], Akihiko Murai[5], Eiichi YOSHIDA[3] and Yoshihiko Nakamura[4], *Member, IEEE*

***Abstract*—Motor functions of the biological system has been forged through 4 billion years evolution. From a neurorobotics view, it is important not only to know how well it works, but also how it fails. To quantitatively describe early onset symptoms of a neurodegenerative disease, we analyzed phenotypes of genetically engineered Huntington disease (HD) model mice, which reveal progressive impaired motor functions. We devised a simple yet sensitive paradigm called the crystalized motion profile (CMP), by which we successfully detected subtle difference between normal and abnormal mice in terms of whole-body level motor coordination. Our long-term objective is to remodel human mind and body to regain impaired motor and cognitive functions with ageing. To do so, we are developing a soft neurorobotic suit that provides integrated cognitive and physical interventions to users. Our analysis on the HD model mice is important as the first step to bridge between molecular mechanisms (altered genetic code) and the macroscopic neuro-musculoskeletal model. With this, we can extrapolate from knowledge of non-human mammals to human to derive the remodeling.**

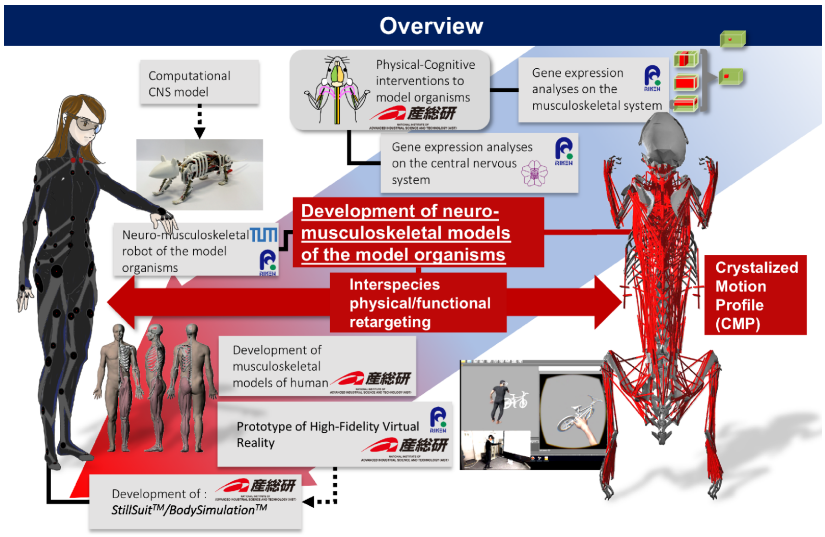

Figure 1. The overview of the ***StillSuit***^{TM} project. Eight subprojects are simultaneously running for its social implementation. ***StillSuit***^{TM} is an endoskeletal robot suit that relies on the endoskeltal system of the human body in terms of the mechanical structure. In this paper, we mainly depict analyses based on "Development of neuro-musculoskeletal models of the model organisms" subproject. "Interspecies physical/functional retargeting" part is separately discussed in [1].The detail of the project will be described in an upcoming project paper.

I. Introduction

In a human-centric (anthropocentrism) view, aging is a slow death and a gradual collapse of the subjective world with decaying psychophysical functions. The aging process was thought to be entirely irreversible [2] [3], especially in the central nervous system (CNS) [4]. Recent studies, however, show that this classical view may need to be revised: the adult brain and neuro-musculoskeletal system are more flexible and dynamic than we believed before. Those studies suggest that it is possible to remodel human mind and body by physical-cognitive interventions, leading to regaining the impaired functions.

Our long-term objective is to reconstruct the decaying 'world' with aging, which everyone has to face someday, through the systematic physical-cognitive interventions (Fig. 1).

We tackle this problem from three different perspectives: biology, robotics, and cognitive sciences. Namely:

*Research supported by KAKENHI (26280110).

[1]Satoshi Oota is with Bioresource Information Division, RIKEN, 3-1-1 Koya-dai, Tsukuba, 305-0074, JAPAN (corresponding author to provide phone: +81-29-836-9039; fax: +81-29-836-9077; e-mail: oota@ riken.jp).

[2]Yuko Okamura-Oho is with Jissen Women's University, 4-1-1 Osakaue, Hino Tokyo 191-8510, Japan (e-mail: yoho-tky@umin.ac.jp).

[3]K. Ayusawa and E. Yoshida are with CNRS-AIST JRL (Joint Robotics Laboratory), UMI3218/RL, Intelligent Systems Research Institute, National Institute of Advanced Industrial Science and Technology, Japan. {k.ayusawa, e.yoshida}@aist.go.jp.

[4]Y. Ikegami and Y. Nakamura are with the Department of Mechano-Informatics, University of Tokyo, Japan (e-mail: [1] K. Ayusawa *et al.*, "Interspecies Retargeting of Homologous Body Posture Based on Skeletal Morphing," presented at the The 2018 IEEE/RSJ International Conference on Intelligent Robots and Systems (IROS 2018), Madrid, Spain, 2018.).

[5]A. Murai is with Human Informatics Research Institute, National Institute of Advanced Industrial Science and Technology, Japan (e-mail: murai@ynl.t.u-tokyo.ac.jp).

1. We elucidate biological mechanisms of remodeling in adult brain-musculoskeletal associated with the physical-cognitive interventions (physical and mental eustresses [5]).
2. Neurorobotics makes it possible to realize mainly physical interventions, as well as mechanical supports/training for the body.
3. The virtual reality is used to provide optimized cognitive interventions, as well as versatile user-friendly interface for the social implementation.

To achieve our goal, we set eight research subjects, each of which deepen and widen its own insights, leading to interdisciplinary fusions to realize the effective social implementation of the *endoskeletal* robot suit, ***StillSuit™*** (Fig. 1 left):

1. Gene expression analyses on the CNS responding to cognitive/physical interventions.
2. Gene expression analyses on the musculoskeletal system responding to physical interventions.
3. Development of neuro-musculoskeletal models of the non-human animals.
4. Development of a neuro-musculoskeletal physical robot of the non-human animals.
5. Development of a neuro-musculoskeletal model of human.
6. Interspecies physical/functional retargeting to bridge between the non-human animals and human neuro-musculoskeletal models.
7. Prototype of High-Fidelity Virtual Reality (Hi-Fi VR) for the cognitive interventions: ***Lucid Virtual Reality***.
8. Development of an endoskeletal robot suit for physical and cognitive interventions: ***StillSuit™***.

As a very beginning step of this project, we apply a neurorobotics approach to analyze phenotypes of genetically modified non-human mammals.

The biological system has substantial robustness and durability against unknown disruptions [6, 7]. Organisms have been repeatedly tested by the harsh environments and been forged through evolutionary processes. Only successful candidates could survive as extant organisms according to Darwinian natural selection [8, 9]. As a consequence, the control system of organisms is so elaborate, versatile, and intelligent.

Due to the biological optimization, meanwhile, the biological control system has a weakness inside: a tiny flaw in the web of genetic interactions can disrupt the whole system, leading to a catastrophic consequence: i.e., "diseases."

One way to design a robust control system is to learn from the biological system and/or mimic it [10]. However, essential understanding of the biological system is notoriously difficult due to the extreme complexity, which was designed by non-human "intelligence:" i.e., evolution.

Biologists have an alternative approach to treat this kind of problem: they intentionally give disturbances to the system and observe their responses to uncover the fundamental mechanism [11, 12]. In other words, biology is a large-scale reverse engineering of the life [13], using a disease as a probe.

In genetics, the disturbance was realized by mutations in the genetic information, which is a blueprint of the life [14, 15]. This molecular-level disturbance is mathematically discrete, and we can identify it with the exact coordinate in the finite genome sequence space [16, 17].

Meanwhile, the response to the disturbance is not that trivial. The response is an entity of the physical world and its possible patterns are virtually infinite [18, 19]. Biologists have often relied on descriptive and/or particular paradigm-dependent manners to handle the responses, which are repeatedly criticized in terms of objectivity, reproducibility and accuracy [20], especially in terms of cognitive and motor functions.

Our basic strategy in order to solve (at least mitigate) the problem is to introduce a constructive neurorobotic approach to the traditional framework. To elucidate the response, we use a neuro-musculoskeletal model to interpret complex biological traits to objective measurements [21]: i.e., we will translate the biological traits to a well-defined tractable problem as done in the preceding studies [22-24], but in a different paradigm.

In this paper, we used a Huntington disease (HD) model mouse, which carries the human HD gene by a transgenic technology. HD is a severe and progressive neurodegenerative disease cause by an abnormal extension of repetitive DNA triplets (CAG) that codes the poly amino acid glutamine (polyglutamine), altering the normal huntingtin (HTT) protein. Its typical symptoms are: dystonia, incoordination, cognitive decline, and behavioral difficulties, typically in middle-age [25]. The number of the CAG repeats is putatively associated with the disease progression.

To elucidate the mechanism of HD, it is significantly important to detect an early onset phenotype (symptom), which was difficult to detect by using conventional frameworks [26]. Our objective is to develop a new framework to detect the early onset phenotypic signal of the HD mice (age 31 days) in terms of the motor functions. Our framework, in turn, will contribute to design an artificial control system to realize robust motor functions.

The significance of the study is to bridge between molecular mechanisms (altered genetic code) and the macroscopic neuro-musculoskeletal model. Regarding our project described above, this is the first step to extrapolate from the knowledge of non-human mammals to human to derive the remodeling.

II. Material and Methods

A. Modeling

Data acquisition for mouse skeletal modeling. Geometry (morphology) of a skeletal model that we used in this paper were based on a set of X-ray CT scanning data obtained by a collaborative work with T. Row [27, 28]. We manually segmented the volume data and modeled joints following a published human model [29]. See Oota et al. (2010) [30] for detailed description.

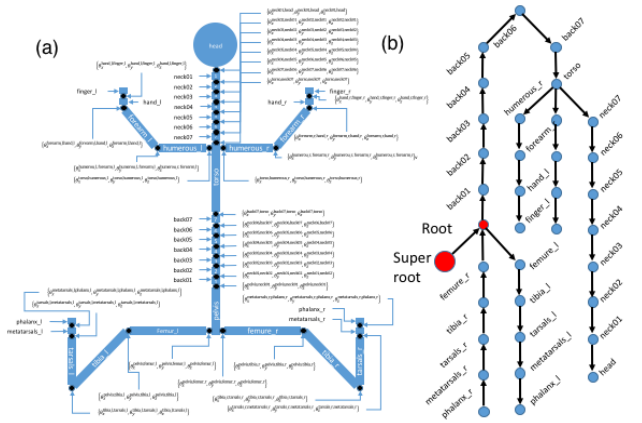

Figure 2. A summary of the joint definitions (a) and the topological sturctue of the mouse skeletal model (b).

Fig. 2 shows a topological structure of the mouse skeletal model. It has a kinematic tree structure whose root is set on the pelvis. Note that the topology has a meta-node (super-root) "ground," which is a parent of the pelvis node. The skeletal model's location (i.e., the global coordinate) is determined by this super-root by giving a displacement from the global origin. We developed the original skeletal model in SIMM (MusculoGraphics, Inc, Chicago, IL) format [30]. We revised the skeletal model in OpenSim XML format after converting it from the SIMM format.

In this paper, we focused on kinematics analyses: i.e., we ignored the mass distribution of the mouse body, which contributes to dynamics. We also omitted the tail form the model for simplicity. This simplification is to decrease the number of parameters which we need to determine through experiments.

Constraints for the vertebra joint. Mouse has 7 cervical bones, 13 thoracic bones, 6 lumber bones, and 4 sacrum bones. If we directly control each joint, the number of parameter would be (30−1)×3=87. Those "back bones" are too complicated for inverse kinematics with our marker set (see section *D*). By giving constraints between joints, we reduced the size of the joint space: i.e., neighboring joints are associated with a simple function [31]. Furthermore, we treated the 13 thoracic bones as one rigid body (see Figs. 2 and 3).

B. Mouse motion capture

We used nine digital cameras (Motion Analysis Corporation, Santa Rosa, CA) to capture mouse motions. Each camera emits infrared lights, and the retroreflective markers on a subject reflect the rays back in the direction of which the rays come in. The sampling rate was 120 Hz. Cortex software (Motion Analysis Corporation, Santa Rosa, CA) was used to reconstruct 3D trajectories of the retroreflective markers. Since obtained motion data were unlabeled (i.e., each marker is not distinguished by the system), we needed to perform "post process" or labeling by using a tool of Cortex and/or by hand. We filmed walking mice with a conventional digital movie camera for the subsequent post process.

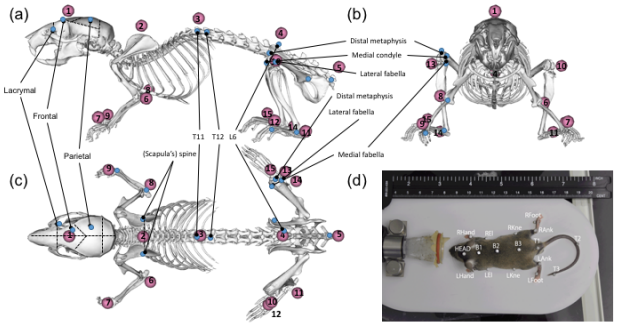

Figure 3. The mouse generic skeletal model and its marker set (a-c). Representative anatomical landmarks are also shown. (d) an actual mouse with markers placed on the skins.

A capture volume (effective space of the motion capture) was calibrated for establishing camera linearization parameters (correction of the lens distortion) such that we achieved approximately 0.2 mm spatial resolution under the given conditions.

The motion capture of mice has particular difficulties described below, and requires special cautions to treat genetically modified animals. We intentionally call this measurement the mouse motion capture (MMC), to distinguish from conventional motion captures.

C. Post process (labeling)

In case of MMC, there are mainly two issues in the post process [27]: (1) motion data are noisier than those of human subjects; (2) motion data are frequently missing due to marker occlusion and proximity. Those are primarily caused by the small size of the subjects [32]. Theoretically speaking, those issue is solvable by increasing the number of cameras to eliminate "blind spots [33]." This approach is, however, leading to an increase of potential cost of experiments. We followed protocols described in the previous works for labeling [27].

D. Mouse marker set

In case of human, there are several established marker sets in clinical applications: e.g., Helen-Hayes (Davis) [34] and

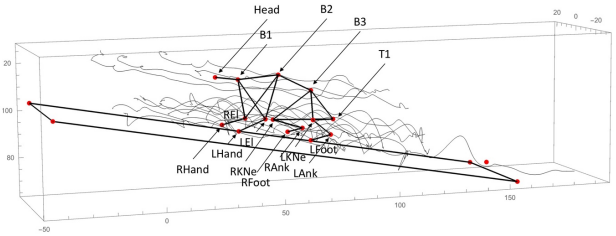

Figure 4. An expected static pose of a mouse on a slope. Red points represent experimental markers (Head, B1, B2, B3, T1, LEl, LHand, REl, RHand, LKne, LAnk, LFoot, RKne, RAnk, and RFoot). The other four markers represent a slope on which the mouse makes gaits. Curve lines indicate trajectories of the experimental markers: i.e., the static pose is the average posture during the gait. The length unit is millimeter. Snapshots of the postures for both healthy and pathological gaits with rendered scaled skeletal models are shown in Fig. 6.

Cleveland clinic marker sets [35]. Unlike human subjects, ratio of maker weight to mouse body weight is inevitable. We developed our own marker set for mouse (MSM) to achieve efficient motion capture with relatively small number of markers (Fig. 3). In this paper, we used 17 optical retroreflective markers assigned to articulated portions of mouse body. Figure 3 shows the marker positions on the mouse skins. We used 2.6 mm retroreflective markers (Motion Analysis Corporation, Santa Rosa, CA). This type of marker is originally used to capture human facial expressions. Marker locations were determined by palpating joint and/or morphological landmark positions. The marker location errors were computationally minimized afterwards (see section *E*). We increased the number of markers by 8 from our previous work [30], owning to lighter markers and higher resolution cameras (Motion Analysis Corporation, Santa Rosa, CA).

E. Static pose computation and scaling

In case of MMC, unlike human and obedient non-human subjects with which we can communicate verbally and/or nonverbally, it is extremely difficult to make mice keep a standardized static pose without stress-prone means. The standardized static pose is important to identify markers as well as standardized inter-marker distances, by which we can perform subject-specific model scaling [36]. We simply took averages of the experimental marker positions during a selected time range, which corresponds to manually segmented motions (Fig. 4). Virtual marker positions were adjusted such that marker errors are minimized by the inverse kinematics [37]. We used virtual markers of pelvis, tibia, and forelimb to adjust the generic model to subjects by affine transformations.

F. Inverse kinematics and marker position optimization

In inverse kinematics (IK), marker positions on skeletal segments are one of important determinants. A subtle deviation of an experimental marker placement site from a corresponding model marker can cause an impact on results of IK. However, it is virtually impossible to exactly assign optical markers to expected landmark positions on mice skins. It is also difficult to model the elasticity of the mouse skins. The marker positions were adjusted in each IK session to minimize the marker errors with equally distributed weights [37, 38].

G. Mouse preparation

We analyzed yeast artificial chromosome (YAC) transgenic mice expressing normal (+) and mutant (Tg) human huntingtin (HTT) in a developmental and tissue specific manner: HD model mouse R6/2 [39]. Totally eight HD mice were used, four of which were normal (+/+) and the others four were abnormal (Tg/+) (see Table I). They were all male and born on the same day (31 days of age). The number of CAG repeats was 120 ± 5. Our experimental protocols, including animals, were approved by the Animal Experiment Committee of the RIKEN Tsukuba Institute.

H. Data analysis

Conventional methods to analyze motor functions rely on spaciotemporal values: e.g., transitions. However, it is obvious that individual variations are so huge in transitions due to "free will," leading to difficulty in reproducibility. A solution to reduce such variations is to spatially restrict a subject: e.g., a forced gait on a treadmill. But this kind of restriction could spoil innate behaviors of the subjects and obscure subtle signals. In addition to that, the restriction has possibilities to alter mechanical properties of the system. In case of the treadmill, for example, effects on the gross inertia of the subject are significantly neglected because it stays in the almost same spatial position.

Our approach is to let subjects behave according to their free will, while we simply focus on dependency between joint angles, eliminating spaciotemporal factors from the motion sequence data. Fig. 5 shows a "dependency tree" of all the joint angle sequences of the motion data 1_4 of Mouse 140912I07. The dependency tree shows, for example, that the knee, ankle, and elbow reveal similar or closely dependent behaviors comparing with the other part of the body. The dependency tree was constructed based on squared Euclidean distances between different motion angle sequences. Our basic idea is that the dependency tree can represent an overall motion profile of the subject in the session.

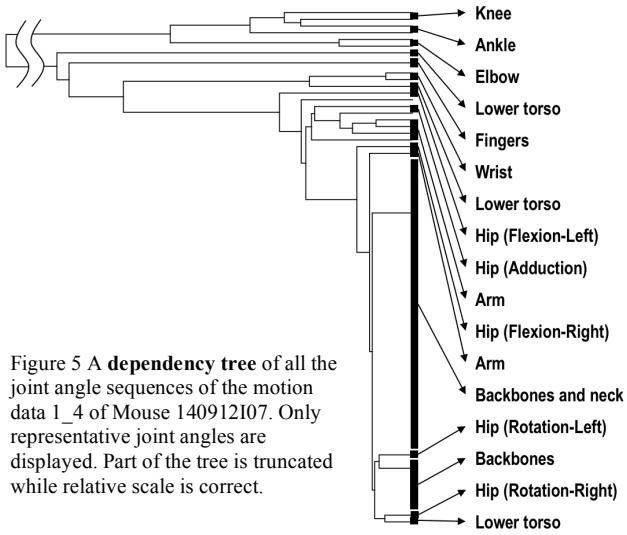

Figure 5 A **dependency tree** of all the joint angle sequences of the motion data 1_4 of Mouse 140912I07. Only representative joint angles are displayed. Part of the tree is truncated while relative scale is correct.

In the actual analysis, we compared all possible pairs of joint angles to generate a huge association matrix to represent the dependency The matrix is regarded as a "crystalized" motion profile (CMP) of a mouse behavior during a session. We directly used CMP matrices in this paper because the topology inference is not always correct depending on the nature of the distance matrix.

Since each element of the matrix is a mare (linear) association, it has no longer spaciotemporal factors in the profile. Here, the motor functions are translated to more primitive and objective entities: linear correlations of different joint angle sequences.

An element of a CMP matrix is defined by the absolute correlation between joint angle sequences of the two different joints i and j:

$$\mathrm{cmp}_{ij} = \frac{1}{m}\left(\sum_{t=1}^{m} \alpha^*_{ti}\alpha_{tj}\right),$$

where $\alpha_{t\,j}$ is an angle of joint j at time step t. $\alpha^*_{t\,j}$ is the conjugate of $\alpha_{t\,j}$. m is the number of time steps. Given a set of joint angle sequences A, we have a CMP matrix as follows:

$$\begin{aligned}
&\mathbf{CMP}(A)\\
&= \{\mathbf{cmp}_{ij}\}\\
&= \begin{pmatrix}
\frac{1}{m}(\alpha_{11}\alpha^*_{11} + \alpha_{21}\alpha^*_{21} + \cdots + \alpha_{m1}\alpha^*_{m1}) & \frac{1}{m}(\alpha_{11}\alpha^*_{12} + \alpha_{22}\alpha^*_{22} + \cdots + \alpha_{m1}\alpha^*_{m2}) & \cdots & \frac{1}{m}(\alpha_{11}\alpha^*_{n} + \alpha_{22}\alpha^*_{2n} + \cdots + \alpha_{m1}\alpha^*_{mn})\\
\frac{1}{m}(\alpha_{12}\alpha^*_{11} + \alpha_{22}\alpha^*_{21} + \cdots + \alpha_{m2}\alpha^*_{m1}) & \frac{1}{m}(\alpha_{12}\alpha^*_{12} + \alpha_{22}\alpha^*_{22} + \cdots + \alpha_{m2}\alpha^*_{m2}) & \cdots & \frac{1}{m}(\alpha_{21}\alpha^*_{n} + \alpha_{22}\alpha^*_{2n} + \cdots + \alpha_{m2}\alpha^*_{mn})\\
\vdots & \vdots & \ddots & \vdots\\
\frac{1}{m}(\alpha_{1n}\alpha^*_{11} + \alpha_{2n}\alpha^*_{21} + \cdots + \alpha_{mn}\alpha^*_{m1}) & \frac{1}{m}(\alpha_{1n}\alpha^*_{12} + \alpha_{2n}\alpha^*_{22} + \cdots + \alpha_{mn}\alpha^*_{m2}) & \cdots & \frac{1}{m}(\alpha_{n}\alpha^*_{n} + \alpha_{2n}\alpha^*_{2n} + \cdots + \alpha_{mn}\alpha^*_{mn})
\end{pmatrix},
\end{aligned}$$

where $A = \{\alpha_{\mathrm{t\,j}}\}$ is a set of joint angles of joint j at time step t. n is the number of joint angles. Note that the size of time steps does not affect dimensions of the CMP matrix.

TABLE I. SUMMARY OF MOTION CAPTURE RESULTS

Mouse ID	Data ID	Genotype	Frame #	Coverage (%)
140912E06	1_1	Tg/+	300	50.00
140912E07	1_2	+/+	88	14.67
140912I06	1_3	+/+	500	83.33
140912I07	1_4	Tg/+	434	72.33
140912G04	1_5	Tg/+	559	93.17
140912L09	1_6	+/+	600	100.00
140912F08	3_3	Tg/+	221	36.83
140912F10	3_4	+/+	546	91.00
Total			3,248	67.67

III. RESULTS

A. HD mouse motion capture

We obtained eight sets of motion data that contain totally 4,800 frames (120 fps), from which we used 3,248 frames for subsequent analyses (Table I). Missing marker data were linearly interpolated by using their flanking frame data if possible. The interpolated data were smoothed by the Butterworth filter [40] with 6 Hz. The gross data coverage of the motion capture was 67.7 %.

Optical markers on mouse skins were occasionally detached during motion capture sessions. In such case, we simply continued the sessions without recovering markers. This is to avoid unexpected influences of anesthesia for the restitution.

In the post process, frequent marker occlusions and noises (ghost markers) were observed. Since Cortex algorithm could not properly handle such noisy data, we manually labeled the makers in those cases. Owning to the small number of markers of our marker set, the labeling was totally deterministic.

Fig. 6 shows snapshots of the postures for healthy (a) and pathological (b) gaits with rendered scaled skeletal models. Marker trajectories are also shown.

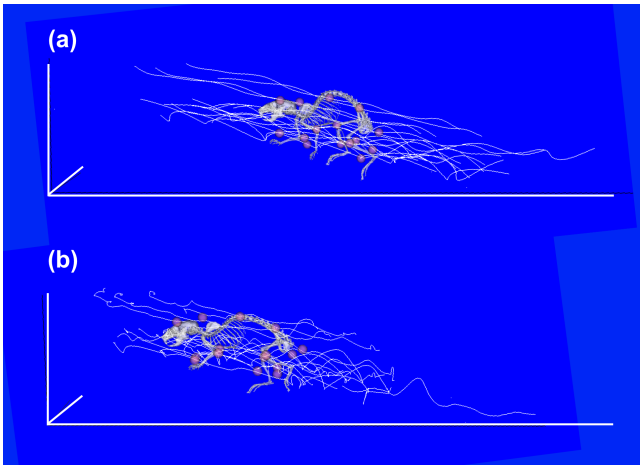

Figure 6. Snapshots of the postures for healthy (a) and pathological (b) gaits and marker trajectories (thin white curves). Pink balls represent virtual markers after adjustments. The global coordinates are represented by thick white lines. We can observe slight differences in the marker trail characteristics between the two subjects.

B. The crystalized motion profiles

We computed the crystalized motion profiles (CMPs) and clustered them by using Agglomerate function of Mathematica [41] according to the squared Euclid distances. An example of the crystalize motion file is shown in Fig. 7. The clustered results were visualized as a dendrogram. Note that the mice are virtually genetically identical except for one

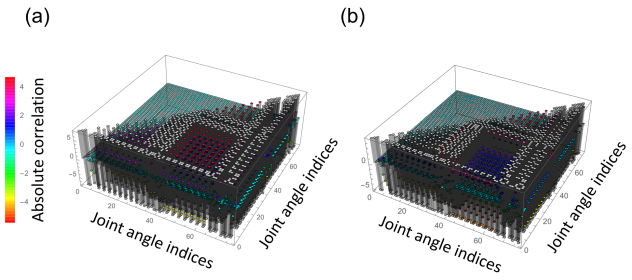

Figure 7. Examples of crystalized motion profiles (CMP). (a) Mouse 140912E07: normal (+/+); (b) Mouse 140912I07: transgenic (Hg/+). While the two examples show visual differences in this particular case, it is generally difficult to distingusih transgenic mice (Tg/+) from the others (+/+) only with visual inspections. Only upper triangular elements are shown because the matrices are symetric.

transgene: human HTT gene and its putatively regulatory regions.

Fig. 8 shows results of the clustering. The mouse motion data were clearly clustered into two groups corresponding to the two genotypes: Tg/+ and +/+ except for data 1_2. Since the probability that randomly sampled mouse motion data have this partition is: $2 \times \frac{8!}{3!(8-3)!} = 0.036$, this partition is significant at 3.6% level. Note that the misclassified data 1_2 has only 88 frames (Table I).

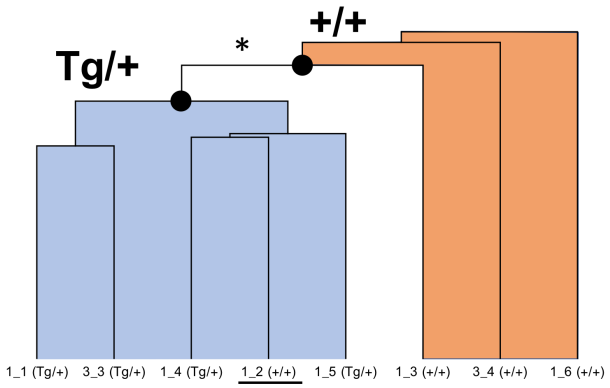

Figure 8. Clustering of mice according to the crystalized motion profile (CMP): Tg/+ and +/+ indicate transgenic and normal mice, respectively. Thick dots represent roots of the clusters. Data 1_2 (Mouse 140912E07) was misclassified (underline). * indicates that the clustering with this edge is significant at 3.6% level.

IV. Discussion and Conclusion

We analyzed motion data of 8 juvenile mice (age of 31 days) that have different genotypes: Tg/+ and +/+. We successfully distinguished their genotypes by using the crystalized motion profile (CMP), except for one case. It is known that HD mice that have Tg/+ genotypes reveal late-onset motor and behavioral difficulties [42]. However, there was no report that CAG 120 HD mice show distinguishable motor and behavioral phenotypes before age of 31 days [43]. It is significant to detect early-onset phenotypic signatures in HD mice to find an effective treatment of HD, as well as to elucidate the neural control mechanism. The CMP made it possible to conducted highly quantitative analyses on mouse motor functions with comprehensive characteristics of motions during a session. This is the first report to detect a quantitative motor phenotypic signature in CAG 120 HD mice at age of 31 days.

Motion data contain various spontaneous signals that are not directly determined by genetic factors [44]. For example, mice can compensate abnormal motions to recover "expected" motor coordination [45]. Such adjustments, however, can obscure genetically determined signatures: i.e., phenotypes. As a result, it can be difficult to detect an early onset phenotype until it gets too severe to compensate by the voluntary adjustments.

Aside from the adaptive internal models, the motion control compensation should occur based on the sensory feedback to correct genetically impaired motor commands [46]. Due to the time lag, the motion data should contain some trace of the corrections.

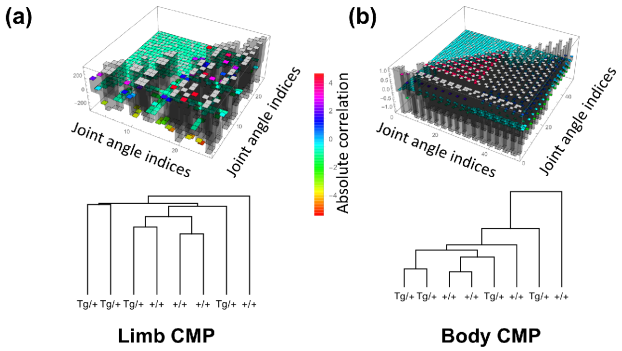

Figure 9. Results obtained from limb CMPs (a) and body CMPs (b) alone. Top: examples of CMPs; bottom: dendrograms that represent classifications of CMPs. They failed to cluster genotypes Tg/+ and +/+.

The problem here is two-fold: (1) we have no prior knowledge when and where the trace can appear; (2) it is virtually impossible to distinguish the genetically essential signature from the voluntary adjustment. Our idea is that, with comprehensive comparison between joint angles, we detect the perceptually hidden signals in the motion data by using high dimensional association matrices: CMP.

There are two advantages on CMP: (1) since CMP has no temporal transition factors of the motion data, sessions that have different durations are directly comparable; (2) the CMP covers the motor coordination of the whole body.

The CMP is, therefore, a comprehensive profile of a session of motions (motion sequences), which is represented by linear associations (dependency) of all possible pairs of joint angles. In a sense, this is a high dimensional representation of complex motion characters mapped to the joint angle space.

In our analyses, we failed to cluster the motion data 1_2 of Mouse 140912E07 (see Table I and Fig. 8). While we still have no conclusive reasons for this misclassification, we should note that the data size of this session is extremely small: 88 frames. This suggests that we need certain amount of motion data for an appropriate clustering.

It is interesting that CMPs of limb and body joints alone failed to lead to expected results (Fig. 9). We also analyzed CMPs between limb and body, excluding CMPs of intra-limb and intra-body joints. Again, we obtained no distinctive partitions between the healthy and pathological gaits (Fig. 10).

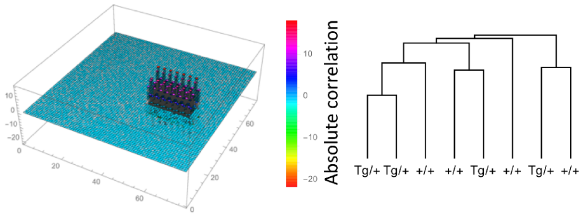

Figure 10. Absolute correlations of CMPs between limb and body, excluding CMPs of intra-limb and intra-body joints. Left: an example of a CMP; Right: a dendrogram that represents classifications of the CMPs. It failed to cluster genotypes Tg/+ and +/+.

They suggest that the impaired motor coordination of HD mice appeared in the associations between the limb and body joints: i.e., the early onset impairs of HD mice are not embedded in the extremities or trunk alone, but in the whole body coordination, at least according to the sensitivity of our method.

The biological "reverse engineering" approach requires a sensitive method to handle complex phenotypes. The CMP is a simple yet sensitive paradigm to express an overall profile of a motion sequence. This paradigm can be a powerful tool to elucidate the biological control system disrupted by specific impairments.

It is well known that the motor coordination of anthropormorphic biped robots in a complex environment is prone to fail [47, 48], revealing "neuro-pathological" traits: e.g., spasm, faint, and stagger-like motions [49, 50]. They are strikingly similar to symptoms observed in neurological disease patients. Many neurological symptoms are caused by slight deviations from the physiological norm, suggesting that acceptable parameter subspace is so tiny comparing with the whole parameter space. Therefore, we can naturally assume that it is extremely difficult to find "optimized" parameter sets in the potentially multimodal parameter space.

In this paper, we used the CMP as a measurement to categorize a population into subpopulations that have different characteristics in motor coordination. On the other hand, we can potentially use the CMP as a kind of *database* (or a lookup table) to decide what kind of motor coordination is appropriated at a certain occasion. For example, we can measure motions of animals (including human) to obtain various CMPs corresponding to different environments: e.g., level ground, staircase, and rugged ground. By querying a joint angle of hip joint, for example, we can quickly retrieve associated joint angles of the other joints with certain correlative coefficients. In other words, we can reduce the aforementioned enormous parameter space without laborious dynamic computations (Fig. 11).

The CMP is potentially useful not only to design controllers of quadruped robots, but also to design humanoid robots, including soft robot suits, like ***StillSuit***™.

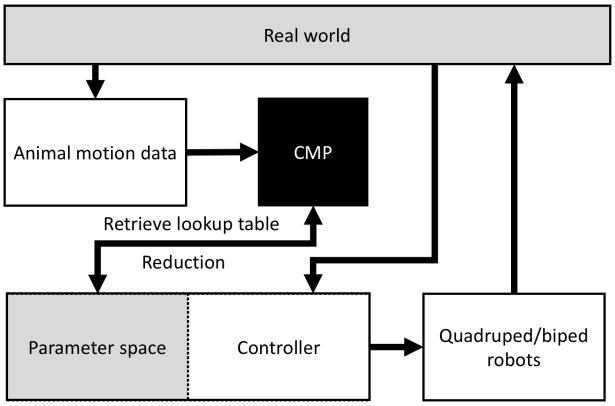

Figure 11. A potential application of the CMP to design a controller for quadruped/biped robots.

To design a robust control system, the bio-inspired approach is expected to be promising. Considering the extreme complexity, however, we should learn from the biological system in terms of not only how well it manages the control, but also how it fails. This kind of disturbance-response analysis will bring us knowledge on the fundamental mechanism which the biological system has acquired for 4 billion years evolution in the harsh natural environment.

More boldly speaking, animals may have a CMP-like lookup table at genetic level, which was forged through the evolution. And if the lookup table is disturbed by genetic defects, it is possible that the animal can no longer coordinate its proper motion, as observed in the HD mice.

The CMP can be a powerful tool in the disturbance-response analysis by using noisy biological data.

ACKNOWLEDGMENT

We appreciate Prof. Rüdiger Dillmann for his insightful advices to improve an early version of our manuscript. We had an inspiration though discussion with Prof. David Franklin. Prof. Miles Pennington hosted a robotics workshop, in which we had a fruitful discussion. Mr. Takumi Yamagishi worked hard for the complex coordination of the project. This work was supported by an internal funding of RIKEN, as well as KAKENHI (26280110).

REFERENCES

[1] K. Ayusawa *et al.*, "Interspecies Retargeting of Homologous Body Posture Based on Skeletal Morphing," presented at the The 2018 IEEE/RSJ International Conference on Intelligent Robots and Systems (IROS 2018), Madrid, Spain, 2018.

[2] A. Murshid, T. Eguchi, and S. K. Calderwood, "Stress proteins in aging and life span," *Int J Hyperthermia,* vol. 29, no. 5, pp. 442-7, Aug 2013.

[3] K. H. Cho, J. I. Joo, D. Shin, D. Kim, and S. M. Park, "The reverse control of irreversible biological processes," *Wiley Interdiscip Rev Syst Biol Med,* vol. 8, no. 5, pp. 366-77, Sep 2016.

[4] S. Grade and M. Götz, "Neuronal replacement therapy: previous achievements and challenges ahead," *npj Regenerative Medicine,* vol. 2, no. 1, p. 29, 2017/10/23 2017.

[5] K. N. Parker and J. M. Ragsdale, "Effects of Distress and Eustress on Changes in Fatigue from Waking to Working," *Appl Psychol Health Well Being,* vol. 7, no. 3, pp. 293-315, Nov 2015.

[6] D. N. Lyttle, J. P. Gill, K. M. Shaw, P. J. Thomas, and H. J. Chiel, "Robustness, flexibility, and sensitivity in a multifunctional motor control model," *Biol Cybern,* vol. 111, no. 1, pp. 25-47, Feb 2017.

[7] Y. Li, G. Dwivedi, W. Huang, M. L. Kemp, and Y. Yi, "Quantification of degeneracy in biological systems for characterization of functional interactions between modules," *J Theor Biol,* vol. 302, pp. 29-38, Jun 7 2012.

[8] C. Darwin, *On the Origin of Species*. Harvard University Press, 1964.

[9] G. G. Dimijian, "Darwinian natural selection: its enduring explanatory power," *Proc (Bayl Univ Med Cent),* vol. 25, no. 2, pp. 139-47, Apr 2012.

[10] S. K. Jha and A. Dass, "Investigative analysis of bio-inspired robust controller for a CNC system," in *2016 3rd International Conference on Computing for Sustainable Global Development (INDIACom)*, 2016, pp. 2471-2475.

[11] J. E. Lee and J. G. Gleeson, "A systems-biology approach to understanding the ciliopathy disorders," *Genome Med,* vol. 3, no. 9, p. 59, Sep 26 2011.

[12] T. Kang, J. T. White, Z. Xie, Y. Benenson, E. Sontag, and L. Bleris, "Reverse engineering validation using a benchmark synthetic gene circuit in human cells," *ACS Synth Biol,* vol. 2, no. 5, pp. 255-62, May 17 2013.

[13] M. V. Rockman, "Reverse engineering the genotype-phenotype map with natural genetic variation," *Nature,* vol. 456, no. 7223, pp. 738-44, Dec 11 2008.

[14] A. S. Bie *et al.*, "Effects of a Mutation in the HSPE1 Gene Encoding the Mitochondrial Co-chaperonin HSP10 and Its Potential Association with a Neurological and Developmental Disorder," *Front Mol Biosci,* vol. 3, p. 65, 2016.

[15] C. Henry, R. Overbeek, and R. L. Stevens, "Building the blueprint of life," *Biotechnol J,* vol. 5, no. 7, pp. 695-704, Jul 2010.

[16] P. A. Gros, H. Le Nagard, and O. Tenaillon, "The evolution of epistasis and its links with genetic robustness, complexity and drift in a phenotypic model of adaptation," *Genetics,* vol. 182, no. 1, pp. 277-93, May 2009.

[17] D. B. Saakian and C.-K. Hu, "Exact solution of the Eigen model with general fitness functions and degradation rates," *Proceedings of the National Academy of Sciences of the United States of America,* vol. 103, no. 13, pp. 4935-4939, 2006.

[18] C. Braendle, C. F. Baer, and M.-A. Félix, "Bias and Evolution of the Mutationally Accessible Phenotypic Space in a Developmental System," *PLoS Genet,* vol. 6, no. 3, p. e1000877, 2010.

[19] J. G. Lomnitz and M. A. Savageau, "Elucidating the genotype-phenotype map by automatic enumeration and analysis of the phenotypic repertoire," *NPJ Syst Biol Appl,* vol. 1, 2015.

[20] A. Capes-Davis and R. M. Neve, "Authentication: A Standard Problem or a Problem of Standards?," *PLoS Biol,* vol. 14, no. 6, p. e1002477, Jun 2016.

[21] Y. Nakamura, K. Yamane, Y. Fujita, and I. Suzuki, "Somatosensory computation for man-machine interface from motion-capture data and musculoskeletal human model," *IEEE Transactions on Robotics,* vol. 21, no. 1, pp. 58-66, 2005.

[22] K. Dana, T. Wataru, and N. Yoshihiko, "Incremental Learning, Clustering and Hierarchy Formation of Whole Body Motion Patterns using Adaptive Hidden Markov Chains," *The International Journal of Robotics Research,* vol. 27, no. 7, pp. 761-784, 2008/07/01 2008.

[23] S. Calinon, F. Guenter, and A. Billard, "On Learning, Representing, and Generalizing a Task in a Humanoid Robot," *IEEE Transactions on Systems, Man, and Cybernetics, Part B (Cybernetics),* vol. 37, no. 2, pp. 286-298, 2007.

[24] M. E. Hussein, M. Torki, M. A. Gowayyed, and M. El-Saban, "Human action recognition using a temporal hierarchy of covariance descriptors on 3D joint locations," presented at the Proceedings of the Twenty-Third international joint conference on Artificial Intelligence, Beijing, China, 2013.

[25] F. O. Walker, "Huntington's disease," *The Lancet,* vol. 369, no. 9557, pp. 218-228.

[26] H. L. Paulson and R. L. Albin, "Huntington's Disease: Clinical Features and Routes to Therapy," in *Neurobiology of Huntington's Disease: Applications to Drug Discovery*, D. C. Lo and R. E. Hughes, Eds.: CRC Press/Taylor & Francis, 2011.

[27] S. Oota *et al.*, "Four-dimensional quantitative analysis of the gait of mutant mice using coarse-grained motion capture," presented at the Engineering in Medicine and Biology Society, 2009. EMBC 2009. Annual International Conference of the IEEE, 2009.

[28] T. Rowe and M. Demarest. (2007, August 11). *"Mus musculus" (On-line), Digital Morphology*. Available: http://digimorph.org/specimens/Mus_musculus/heterozygous/juvenile/whole/

[29] Y. Nakamura, K. Yamane, and A. Murai, "Macroscopic Modeling and Identification of the Human Neuromuscular Network," *in Proc. of the IEEE EMBS '06 28th Annual International Conference,* pp. 99-105, 2006.

[30] S. Oota *et al.*, "Development of a coarse-grained skeletal model of laboratory mouse and its biomechanical applications," presented at the 1st International Conference on Applied Bionics and Biomechanics (ICABB-2010), VENICE, ITALY, OCTOBER 15, 2010. Available: http://www.icabb-iss.org/

[31] M. Christophy, N. A. Faruk Senan, J. C. Lotz, and O. M. O'Reilly, "A musculoskeletal model for the lumbar spine," *Biomech Model Mechanobiol,* vol. 11, no. 1-2, pp. 19-34, Jan 2012.

[32] D. P. Gibson, D. J. Oziem, C. J. Dalton, and N. W. Campbell, "A system for the capture and synthesis of insect motion," *Graph. Models,* vol. 69, no. 5-6, pp. 231-245, 2007.

[33] P. Eichelberger *et al.*, "Analysis of accuracy in optical motion capture - A protocol for laboratory setup evaluation," *J Biomech,* vol. 49, no. 10, pp. 2085-8, Jul 5 2016.

[34] T. D. Collins, S. N. Ghoussayni, D. J. Ewins, and J. A. Kent, "A six degrees-of-freedom marker set for gait analysis: repeatability and comparison with a modified Helen Hayes set," *Gait Posture,* vol. 30, no. 2, pp. 173-80, Aug 2009.

[35] B. Svoboda and A. Kranzl, "A study of the reproducibility of the marker application of the Cleveland Clinic Marker Set including the Plug-In Gait Upper Body Model in clinical gait analysis," *Gait & Posture,* vol. 36, pp. S62-S63.

[36] N. Neave, K. McCarty, J. Freynik, N. Caplan, J. Honekopp, and B. Fink, "Male dance moves that catch a woman's eye," *Biol Lett,* vol. 7, no. 2, pp. 221-4, Apr 23 2011.

[37] S. L. Delp *et al.*, "OpenSim: open-source software to create and analyze dynamic simulations of movement," *IEEE Trans Biomed Eng,* vol. 54, no. 11, pp. 1940-50, Nov 2007.

[38] C. R. Andersen, "Determination of rigid body registration marker error from edge error," *J Biomech,* vol. 42, no. 7, pp. 949-51, May 11 2009.

[39] L. Mangiarini *et al.*, "Exon 1 of the HD gene with an expanded CAG repeat is sufficient to cause a progressive neurological phenotype in transgenic mice," *Cell,* vol. 87, no. 3, pp. 493-506, Nov 1 1996.

[40] S. Butterworth, "On the Theory of Filter Amplifiers," *Experimental Wireless and the Wireless Engineer,* vol. 7, pp. 536-541, 1930.

[41] I. Wolfram Research, "Mathematica," Version 11.0 ed. Champaign, Illinois: Wolfram Research, Inc., 2016.

[42] W. Yang and G. M. X, "Mouse Models for Validating Preclinical Candidates for Huntington's Disease," in *Neurobiology of Huntington's Disease: Applications to Drug Discovery*, L. DC and H. RE, Eds.: Boca Raton (FL): CRC Press/Taylor & Francis, 2011.

[43] M. Wegrzynowicz *et al.*, "Novel BAC Mouse Model of Huntington's Disease with 225 CAG Repeats Exhibits an Early Widespread and Stable Degenerative Phenotype," *J Huntingtons Dis,* vol. 4, no. 1, pp. 17-36, 2015.

[44] M. Hallett, "Volitional control of movement: the physiology of free will," *Clin Neurophysiol,* vol. 118, no. 6, pp. 1179-92, Jun 2007.

[45] L. Collin, A. Usiello, E. Erbs, C. Mathis, and E. Borrelli, "Motor training compensates for cerebellar dysfunctions caused by oligodendrocyte ablation," *Proc Natl Acad Sci U S A,* vol. 101, no. 1, pp. 325-30, Jan 6 2004.

[46] R. Shadmehr, M. A. Smith, and J. W. Krakauer, "Error correction, sensory prediction, and adaptation in motor control," *Annu Rev Neurosci,* vol. 33, pp. 89-108, 2010.

[47] S. Aoi, P. Manoonpong, Y. Ambe, F. Matsuno, and F. Worgotter, "Adaptive Control Strategies for Interlimb Coordination in Legged Robots: A Review," *Front Neurorobot,* vol. 11, p. 39, 2017.

[48] P. Manoonpong, T. Geng, T. Kulvicius, B. Porr, and F. Worgotter, "Adaptive, fast walking in a biped robot under neuronal control and learning," *PLoS Comput Biol,* vol. 3, no. 7, p. e134, Jul 2007.

[49] E. Guizzo and E. Ackerman. (2015). *DARPA Robotics Challenge: A Compilation of Robots Falling Down*. Available: https://spectrum.ieee.org/automaton/robotics/humanoids/darpa-robotics-challenge-robots-falling

[50] J. Nassour, V. Hugel, F. Ben Ouezdou, and G. Cheng, "Qualitative adaptive reward learning with success failure maps: applied to humanoid robot walking," *IEEE Trans Neural Netw Learn Syst,* vol. 24, no. 1, pp. 81-93, Jan 2013.